A Decision Tool based on a Multi-Objective Methodology for designing High-Pressure Thermal Treatments in Food Industry

Miriam R. Ferrández[a,1], Juana L. Redondo[a], Benjamin Ivorra[b], Ángel M. Ramos[b], Pilar M. Ortigosa[a]

[a] *Dept. de Informática, Universidad de Almería, ceiA3, Ctra. Sacramento, La Cañada de San Urbano, 04120 Almería, Spain*
[b] *Instituto de Matemática Interdisciplinar (IMI) & Dept. de Matemática Aplicada, Universidad Complutense de Madrid, Plaza de las Ciencias, 3, 28040 Madrid, Spain*

Abstract

In this work, we propose a methodology for designing High-Pressure Thermal processes for food treatment. This approach is based on a multi-objective preference-based evolutionary optimization algorithm, called WASF-GA, combined with a decision strategy which provides the food engineer with the best treatment in accordance with some quality requirements. The resulting method is compared to a mono-objective optimization algorithm called MLS-GA. To do so, we consider several particular mono-objective and multi-objective optimization problems. Then, considering those cases, we determine an adequate set of parameters for the WASF-GA and the MLS-GA algorithms in order to obtain a reasonable compromise between solution quality and computational time. Next, we compare the results obtained by the WASF-GA and MLS-GA. Additionally, the best solutions returned by the WASF-GA are analyzed from a food engineering point of view. Finally, a sensitivity analysis regarding the impact of design parameters on the performances of those solutions is performed.

Keywords: Decision Support System, Genetic algorithms, Metaheuristics, Food Industry, High-Pressure

1. Introduction

High-Pressure (HP) technology is widely used in food treatment processes [1]. In the last decades, its popularity has grown significantly due to the increasing demand for healthy and safe products, minimally processed, and at the

Email addresses: mrferrandez@ual.es (Miriam R. Ferrández), jlredondo@ual.es (Juana L. Redondo), ivorra@mat.ucm.es (Benjamin Ivorra), angel@mat.ucm.es (Ángel M. Ramos), ortigosa@ual.es (Pilar M. Ortigosa)
[1] Corresponding author.

same time, ready for immediate consumption. Among other food treatments, HP stands out for the two following advantages: it does not use additives that consumers prefer to avoid, and it is not based on extremely high or low temperatures, which can affect nutritional and organoleptic properties of the food.

Regarding existing literature, several food treatment techniques have already been studied and improved by means of optimization methods. For instance, in [2, 3], a food thermal sterilization process is improved in order to find the best heating temperature profile maximizing the organoleptic properties retention and maintaining a specified microbiological lethality. In [4], a multi–objective genetic algorithm is employed to minimize the residual activity and maximize the mass flow rate subject to some temperature constraints of a pulse electric field process for liquid food. As a final example, in [5, 6], a response surface methodology is applied for optimizing a high hydrostatic pressure process with the objective of minimizing different micro-organism activities and maximizing the retention of beneficial properties and quality indicators.

Frequently, optimization problems in food treatment involve several conflicting objectives which must be tackled simultaneously. In multi-objective optimization, there is usually no single optimal solution, but a set of alternative results with different trade-offs. Such a set of solutions is called the Pareto set (or efficient set), and the corresponding set of objective vectors, the Pareto front. Despite the existence of multiple Pareto optimal solutions, in practice, only one of these solutions is selected and applied. This task is carried out by the Decision Maker (DM), i.e. a person who wants to solve the problem and decides which Pareto optimal solution satisfies his/her preferences more suitably.

Analyzing the complete approximation of the Pareto front poses an important challenge to the DM since he/she may be unable to revise all the obtained solutions and to select the best one without any support of interactive methods. Therefore, during the last decade, there has been an active development of Preference-based Multi-objective Evolutionary Algorithms (PMOEAs) to help DMs carry out their tasks. The main aim of PMOEAs is to find an approximation of the Pareto front whose elements are scattered according to the preference information provided by the DM. Among all the PMOEAs [7, 8, 9], the ones based on preference information, and in particular those approaches in which the information is provided by means of a reference point (RP), are the most developed and widely used, mainly due to their inherent meaning. An RP is a point in objective space defined by a DM and indicates his/her desire levels for the objective functions.

Although many different PMOEAs have been developed, as far as we know, the Weighting Achievement Scalarizing Function Genetic Algorithm (WASF-GA) [10] is the most accurate to deal with problems with three or more objective functions.

In this work, we focus on a particular food treatment device (a cylindrical chamber) which is used to apply a combination of High-Pressure and Thermal processes to treat food samples. We model the behavior of this device by considering the heat transfer equations, to model the variations of pressure and temperature, coupled with a first–order kinetic equation, that describes the ef-

fect of such variations on the activity of certain enzymes and vitamins [11]. Consequently, given the pressure profile and the initial and refrigeration temperature, this model simulates the variation of temperatures and the evolution of enzymatic and vitamin activities in the food sample. Then, based on this mathematical model, we define a multi–objective optimization problem, associated to this High-Pressure Thermal treatment, which consists of determining the initial and refrigeration temperatures and the pressure profile provided to the equipment in order to minimize the final enzymatic activity and the maximum temperature reached during the whole process and to maximize the final vitamin activity. To solve this optimization problem, taking into account that in this kind of problem we are only interested in a subset of the possible optimal solutions close to some reference values, we have used the preference–based algorithm called WASF-GA to lead the search towards the region of interest and, thus, avoiding unnecessary computations. Once the solution set of WASF-GA is obtained, we propose to apply a decision approach which provides the decision maker with the most suitable point between all the approximate Pareto optimal front solutions according to some prescribed quality requirements (here, the final vitamin and enzymatic activities and the maximum temperature reached during the treatment), without having to execute any additional optimization procedure. This methodology is analyzed for different settings of parameters for the WASF-GA algorithm by considering two particular mono-objective optimization problems. Then, its capacity to solve those cases is compared with the solutions returned by a hybrid mono-objective algorithm, called MLS-GA. Next, we analyze the solutions returned by the WASF-GA from a food engineering point of view. Finally, we perform a brief sensitivity analysis of the obtained decision parameters in order to give recommendations to practitioners when implementing those kinds of results.

This article is organized as follows. In Section 2, we present the mathematical models used to simulate the High-Pressure Thermal process and its effects on some biological entities' activities inside a food sample. In Section 3, we detail the optimization methodologies that are employed to solve the optimization problems defined in Section 4. Additionally, in Section 4, all the parameters required to reproduce the considered numerical experiments are specified, including those involved in the mathematical model and in the optimization algorithms. Then, in Section 5, the numerical results obtained for the mono-objective optimization problems using the proposed methodology and the mono-objective algorithm are discussed and compared between them. We also perform an implementation study and a sensitivity analysis of the obtained decision variables. Finally, the conclusions are summarized in Section 6.

2. Mathematical modelling of High-Pressure Thermal processes

In High-Pressure Thermal (HPT) processes, food is packed and introduced into a high-pressure equipment, usually with a hollow steel cylinder [11]. This cylinder is filled with a pressurizing fluid, which is generally water. The equipment is able to increase or decrease the pressure of this fluid according to a given

pressure temporal evolution. As a consequence of the compression/expansion, the temperature inside the vessel, and thus the food sample, experiment some changes [12, 13, 14]. To control those thermal variations, the boundary of the vessel can be cooled or warmed during the process [15]. At the end of the process, the fluid vessel is emptied and the packed food is moved out, ready for consumption.

In this section, we are interested in modelling the effects of such HPT treatments on some biological activities inside a particular food sample. To do so, we consider a cylindrical vessel of height H and radius L, which presents axial symmetry. Thus, it can be described by a two-dimensional domain consisting of half of its cross section. More precisely, let $\Omega = [0, L] \times [0, H]$ be the computational domain (see Figure 1), where we distinguish the sub-domain occupied by the food sample, denoted by Ω_{F}; the one corresponding to the sample holder rubber cap, Ω_{C}; the one that contains the pressurizing fluid, Ω_{P}; and the surrounding sub-domain made of steel, Ω_{S}. Additionally, we consider a refrigeration boundary, denoted by $\Gamma_{\mathrm{r}} \subset \{L\} \times \{0, H\}$, whose temperature is set to T_{r} during the whole treatment (see Figure 1). On the upper boundary, denoted by $\Gamma_{\mathrm{up}} = \{0, L\} \times \{H\}$, there is a certain heat transfer with the room. Finally, the remaining boundaries are thermally isolated.

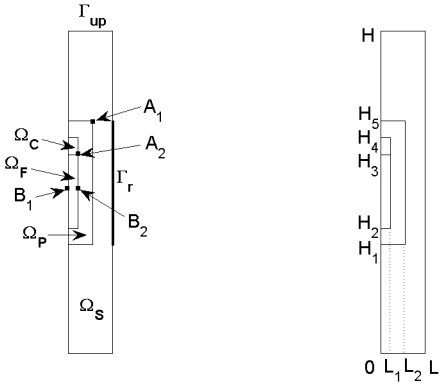

Figure 1: Computational domain Ω: **(Left)** Considered sub-domains, boundaries and points; **(Right)** Typical lengths.

In this work, we suppose that the food is solid and that the filling ratio of the food sample inside the vessel is much higher than the one of the pressurizing medium [11]. Under those assumptions, following [13], the convection phenomenon inside the pressurizing fluid can be neglected. Thus, using cylindrical coordinates in our computational domain, the evolution of the temperature

in the cylinder is governed by the following heat transfer system:

$$\begin{cases} \rho C_p \dfrac{\partial T}{\partial t} - \dfrac{1}{r}\dfrac{\partial}{\partial r}\left(rk\dfrac{\partial T}{\partial r}\right) - \dfrac{\partial}{\partial z}\left(k\dfrac{\partial T}{\partial z}\right) = \alpha \dfrac{\mathrm{d}P}{\mathrm{d}t} T & \text{in} \quad \Omega \times (0, t_\mathrm{f}), \\ k\dfrac{\partial T}{\partial \mathbf{n}} = 0 & \text{on} \quad \Gamma \backslash (\Gamma_\mathrm{r} \cup \Gamma_\mathrm{up}) \times (0, t_\mathrm{f}), \\ k\dfrac{\partial T}{\partial \mathbf{n}} = h(T_\mathrm{amb} - T) & \text{on} \quad \Gamma_\mathrm{up} \times (0, t_\mathrm{f}), \\ T = T_\mathrm{r} & \text{on} \quad \Gamma_\mathrm{r} \times (0, t_\mathrm{f}), \\ T(0) = T_0 & \text{in} \quad \Omega, \end{cases} \tag{1}$$

where t_f is the final treatment time in seconds (s); $T = T(t)$ is the temperature in K and $P = P(t)$ is the pressure in Pa applied by the equipment at time t; $\rho = \rho(T, P)$ in $\mathrm{Kg\,m^{-3}}$ is the density; $C_p = C_p(T, P)$ is the heat capacity in $\mathrm{J\,Kg^{-1}K}$; $k = k(T, P)$ in $\mathrm{W\,m^{-1}K^{-1}}$ is the thermal conductivity; $\alpha = \alpha(T, P)$ in $\mathrm{K^{-1}}$ is the thermal expansion coefficient for the food in the domain Ω_F or for the pressurizing fluid in Ω_P; $\mathbf{n}$ is the outward unit normal vector in the boundary of the domain; T_0 is the initial temperature; T_amb is the ambient temperature; and h is the heat transfer coefficient in $\mathrm{W\,m^{-2}K^{-1}}$. A mathematical analysis of this HPT model was carried out in [16].

The effects of a pressure P and a temperature T on the activity of certain biological entities (such as enzymes or vitamins) can be described combining the Arrhenius and Eyring equations (see, e.g., [17]) to define their inactivation rate as

$$\kappa(P, T) = \kappa_\mathrm{ref} \exp\left(-B\left(\frac{1}{T} - \frac{1}{T_\mathrm{ref}}\right)\right) \exp\left(-C(P - P_\mathrm{ref})\right), \tag{2}$$

where T_ref in K and P_ref in MPa are reference values for the temperature and the pressure, respectively; κ_ref in $\mathrm{min^{-1}}$ is the inactivation rate at these reference conditions; B in K and C in $\mathrm{MPa^{-1}}$ are the temperature dependence and the pressure dependence parameters of κ, respectively.

This inactivation rate allows us to define the temporal evolution of the activity $A(t)$ (characterized as the percent value of the initial activity) of a studied biological entity by considering the following first–order kinetic equation:

$$\frac{\mathrm{d}A}{\mathrm{d}t}(t) = -\kappa(P(t), T(t))\, A(t), \tag{3}$$

with $A(0)$=1; and $P(\cdot)$ and $T(\cdot)$ functions modelling the temporal variation of the pressure and temperature, respectively.

In order to describe the evolution of the non–homogeneous activity distribution inside the food sample during the process, the previous heat transfer model (1) has to be coupled with Equation (3). To this aim, we consider that the particles of solid type food are motionless and that the mass transfer pressure

is negligible compared to the equipment pressure [11]. Thus, the activity A of a particle located at a point $(r, z) \in \Omega_{\mathrm{F}}$ at time t is given by

$$A(r, z, t) = A(r, z, 0) \exp\left(- \int_0^t \kappa(P(\sigma), T(r, z, \sigma)) \mathrm{d}\sigma \right), \tag{4}$$

where $A(\cdot, \cdot, 0) = 1$; $P(\cdot)$ is the equipment pressure provided by the user; and T is the temperature obtained by solving System (1).

We note that these models have been successfully applied when studying the inactivation of various enzymes with different conditions of pressure and temperature (see, e.g., [18] and [19]).

3. Optimization methodologies

In this section, we highlight two optimization methodologies that will be used to solve the mono-objective and multi-objective optimization problems presented in subsection 4.3 and subsection 4.2. First, in subsection 3.1, we introduce general formulations of global and multi-objective optimization problems and recall some classical definitions to be used in the present work. Then, in subsection 3.2, two particular approaches are described in order to tackle those general optimization problems. Subsection 3.3 is devoted to introducing WASF-GA. Next, in subsection 3.4, we explain an original methodology that consists of using WASF-GA for solving mono-objective problems. Finally, subsection 3.5 introduces a multi-layer secant genetic algorithm for mono-objective problems.

3.1. Theoretical framework

In this work, we focus on optimizing single objective or several objectives simultaneously. In the former case, we deal with *global optimization* problems [20], whereas the latter leads to *multi-objective optimization* problems [21].

On the one hand, the aim of *global optimization* is to find the best (i.e. global) solution of optimization problems, in the presence of local and global optimal solutions. The formulation of a global optimization problem, in its minimization form, can be represented by:

$$\begin{array}{ll} \min & f(\mathbf{x}) \\ \text{s. t.} & \mathbf{x} \in S \subseteq \mathbb{R}^n, \end{array} \tag{5}$$

where S is a non-empty set in $\mathbb{R}^n$, called feasible space, and f is a real valued function called objective function.

On the other hand, in general, a *multi-objective optimization* problem can be formulated as follows:

$$\begin{array}{ll} \{\min f_1(\mathbf{x}), \ldots, \min f_m(\mathbf{x})\} \\ \text{s.t.} \quad \mathbf{x} \in S \subseteq \mathbb{R}^n \end{array} \tag{6}$$

where $S \subseteq \mathbb{R}^n$ is the *feasible region* of *decision vectors* $\mathbf{x} = (x_1, \ldots, x_n)$, with $n \in \mathbb{N}$, and $f_1, \ldots, f_m : \mathbb{R}^n \longrightarrow \mathbb{R}$ are the *objective functions*. The m-dimensional

image vectors $\mathbf{f}(\mathbf{x}) = (f_1(\mathbf{x}), \ldots, f_m(\mathbf{x}))$ are referred to as *objective vectors* and the image of the feasible set in the objective space $\mathbb{R}^m$ is called the *feasible objective region* $Z = \mathbf{f}(S)$.

When there are several objectives to deal with, a unique solution that minimizes all the objectives at the same time does not always exist. Frequently, the different objectives contradict each other and the solution consists of several trade-off points of the feasible space.

Definition 1. For two feasible vectors $\mathbf{x}, \mathbf{x}' \in S$, we say that $\mathbf{x}$ *dominates* $\mathbf{x}'$ and $\mathbf{f}(\mathbf{x})$ dominates $\mathbf{f}(\mathbf{x}')$ if and only if $f_i(\mathbf{x}) \leq f_i(\mathbf{x}')$ for all $i = 1, \ldots, m$, and there exists one $j \in \{1, \ldots, m\}$ such that $f_j(\mathbf{x}) < f_j(\mathbf{x}')$.

Definition 2. A decision vector $\mathbf{x} \in S$ is said to be *efficient* or *a Pareto optimal solution* if and only if there does not exist another feasible vector $\mathbf{x}' \in S$ dominating $\mathbf{x}$, i.e., none of the objective functions can be improved without worsening at least one of the others. The set S_E of all the Pareto optimal solutions is called the *efficient set* or the *Pareto optimal set*. The image of a Pareto optimal solution $\mathbf{f}(\mathbf{x})$ is called *Pareto optimal objective vector* and the set of all the Pareto optimal objective vectors $\mathbf{f}(S_E)$ is denominated *Pareto optimal front*.

Thus, solving a multi-objective optimization problem consists of finding the nondominated subset formed by the efficient decision vectors whose corresponding objective vectors represent the Pareto optimal front.

An upper and a lower bounds for this Pareto optimal front can be established by means of the nadir and the ideal objective vectors, respectively, as explained below.

Definition 3. The *nadir objective vector* $\mathbf{z}^{\text{nad}} = (z_1^{\text{nad}}, \ldots, z_m^{\text{nad}})$ is defined as the vector with the worst values that the objective functions can reach in the Pareto optimal front. Conversely, the *ideal objective vector* $\mathbf{z}^* = (z_1^*, \ldots, z_m^*)$ is composed of the best values that each objective function can achieve in the Pareto optimal front. Therefore, each component of these vectors can be obtained as $z_i^{\text{nad}} = \max_{\mathbf{x} \in S_E} f_i(\mathbf{x})$, $z_i^* = \min_{\mathbf{x} \in S_E} f_i(\mathbf{x})$, for all $i = 1, \ldots, m$, respectively.

3.2. Considered approaches to deal with the optimization problems

Solving (6) means obtaining the whole efficient set, that is, all the points which are efficient, and its corresponding Pareto front. However, for a majority of multi-objective problems, obtaining an exact description of the efficient set (or Pareto front) is practically impossible, since those sets are usually a continuum and include an infinite number of points. Furthermore, the computing cost may be excessive, and this is an important aspect, mainly for hard-to-solve optimization problems, such as the one considered in this work.

At this point, there exist two possibilities to deal with Problem (6): (i) Reduce the multi-objective problem to a constrained mono-objective optimization problem of the form (5), whose resolution procedure is less time consuming.

However, it provides a unique minimum point and hence, each time the thresholds of some of the constraints are changed, a new optimization problem has to be solved. (ii) Use PMOEAs, which allow us to obtain 'good approximations' of the region of interest (ROI) in reasonable computing times. A good *Pareto front approximation* is defined as a finite set of non-dominated objective vectors which cover the whole ROI evenly. Therefore, once the Pareto front approximation is computed, the decision maker has available a set of points that are individually good solutions for many different constrained mono-objective problems. Then, the DM can choose the most preferable one depending on the specific quality requirements that he/she wants to satisfy at each moment without having to execute a new optimization procedure.

In this work, this methodology is analyzed by means of two algorithms: WASF-GA and MLS-GA.

WASF-GA was proposed in [10]. Currently, this is the reference algorithm in the PMOEA community since it is the most effective method for optimization problems with three or more objectives. Additionally, it is one of the few methods able to obtain well-distributed solutions covering the complete ROI [10]. For these reasons, it will be used to deal with the problem at hand.

MLS-GA is a hybrid mono-objective methodology which is based on a genetic algorithm (GA) as a main strategy combined with a multi–layer secant (MLS) technique and a Steepest Descent (SD) algorithm. MLS was introduced in [22] and it is demonstrated to be a good line search method for providing a good initial population. Additionally, SD is used as a local optimizer in order to improve the quality of the solution.

3.3. The Weighting Achievement Scalarizing Function Genetic Algorithm

This subsection is devoted to explaining the fundamentals of WASF-GA. For more details, the interested reader is referred to [10].

A general scheme of WASF-GA is shown in Algorithm 1. In WASF-GA, the DM must provide, as input parameter, a desirable value q_i for each one of the objective functions f_i, with $i = 1, \ldots, m$. All these values constitute the reference point $\mathbf{q} = (q_1, \ldots, q_m)$. Notice that such a reference point can be achievable or unachievable, depending on whether it belongs to the feasible objective region $\mathbf{f}(S)$ or not. As can be seen in Figure 2, if $\mathbf{q}$ is achievable, the region of interest is composed by the objective vectors that dominate $\mathbf{q}$, i.e. the Pareto optimal objective vectors $\mathbf{f}(\mathbf{x})$ with $\mathbf{x} \in S_E$ verifying $f_i \leq q_i$, for all $i = 1, \ldots, m$. In contrast, if $\mathbf{q}$ is unachievable, the region of interest will be formed by the Pareto optimal objective vectors that are dominated by $\mathbf{q}$, i.e. $\mathbf{f}(\mathbf{x})$ with $\mathbf{x} \in S_E$ satisfying $f_i \geq q_i$, for all $i = 1, \ldots, m$.

In addition to the reference point, a parameter $\eta > 0$ and a sample of weight vectors $\{\mu^1, \ldots, \mu^{N_\mu}\}$ should be provided. The parameter η, called augmentation coefficient, must be a small positive value. Its objective is to guarantee the equivalence between problems (6) and (7). Each weight vector μ^j, with $j = 1, \ldots, N_\mu$, is equal to $\mu^j = (\mu^j_1, \ldots, \mu^j_m)$, where $\mu^j_i > 0$ and $i = 1, \ldots, m$. At each generation, $\mathbf{q}$ is projected onto the optimal front in the direction given by

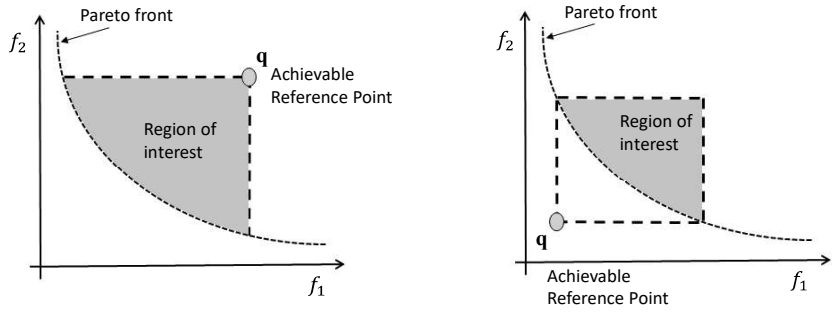

Figure 2: Region of interest: (left) achievable reference point and (right) unachievable reference point.

the inverses of the weights. Consequently, in order to obtain a well-distributed approximation of the region of interest, the sample of weight vectors must be selected so that the inverse of its components μ_i^j must be evenly distributed in the space $(0,1)^m$.

Finally, the number $h_{\max}$ of generations and the number N of individuals in the population, at each generation, must also be set. Notice that the number of function evaluations consumed by WASF-GA is equal to $N \cdot h_{\max}$.

WASF-GA is based on the use of an achievement scalarizing function (ASF). In particular, it uses Wierzbicki's ASF, which is based on the L_∞ distance:

$$s(\mathbf{q}, \mathbf{f}(\mathbf{x}), \mu^j) = \max_{i=1,\ldots,m} \{\mu_i^j (f_i(\mathbf{x}) - q_i)\} + \eta \sum_{i=1}^{m} \mu_i^j (f_i(\mathbf{x}) - q_i),$$

Then, the original multi-objective problem (6) is transformed into the following mono-objective optimization problem:

$$\begin{array}{ll} \min & s(\mathbf{q}, \mathbf{f}(\mathbf{x}), \mu^j) \\ \text{s. t.} & \mathbf{x} \in S \subseteq \mathbb{R}^n. \end{array} \tag{7}$$

Broadly speaking, the algorithm proceeds as follows. Initially, a population P of N individuals is generated. At each generation h, a new offspring Q is generated by applying mutation and crossover operators. These new individuals are inserted in the population list (Step 2-5 in Algorithm 1). Then, all individuals are classified into different fronts. Each front is formed by the solutions with the lowest values of the ASF for the different weight vectors in the set (Steps 6-16). Finally, the most preferable solutions are selected to be part of the population at the next generation (Steps 17-22).

Algorithm 1 WASF-GA ($\mathbf{q}$, $\mathbf{f}$, $\{\mu^1, \ldots, \mu^{N_\mu}\}$,$\eta$, N, $h_{\max}$)

Set $h = 0$, $P^0 =$ population of N randomly generated individuals
while $h < h_{\max}$
    Set $Q =$ population of N offsprings generated from P^h applying mutation and crossover
    $P = P^h \cup Q$
    for every feasible $\mathbf{x} \in P$ ▷ *Classification of the individuals into fronts*
        for $j = 1, \ldots, N_\mu$
            Calculate $s(\mathbf{q}, \mathbf{f}(\mathbf{x}), \mu^j)$
    Set $n = 1$
    while there are unclassified feasible individuals $\mathbf{x} \in P$
        for $j = 1, \ldots, N_\mu$
            $\mathbf{x}^j$ such that $s(\mathbf{q}, \mathbf{f}(\mathbf{x}^j), \mu^j) = \min_{\mathbf{x} \in P, \mathbf{x} \text{ feasible}} s(\mathbf{q}, \mathbf{f}(\mathbf{x}), \mu^j)$
            Add $\mathbf{x}^j$ into F_n^h
            Remove $\mathbf{x}^j$ temporarily from P
        $n = n + 1$
    Classify infeasible solutions according to their overall constraints violation
    Set $P^{h+1} = \emptyset$, $n = 1$ ▷ *Selection*
    while $\mid P^{h+1} \cup F_n^h \mid \leq N$
        $P^{h+1} = P^{h+1} \cup F_n^h$
        $n = n + 1$
    while $\mid P^{h+1} \mid < N$
        Add $\mathbf{x} \in F_n^h$ such that has the lowest values of s into P^{h+1}
    $h = h + 1$
return F_1^h

3.4. Solving mono-objective problems with WASF-GA

Here, our proposal is to solve mono-objective problems as the one formulated in (5) using the Pareto front approximation obtained as an outcome of (6).

Algorithm 2 receives the mono-objective function f, the feasible set S and the set of individuals $\{\mathbf{x}_1, \mathbf{x}_2, \ldots, \mathbf{x}_N\}$ belonging to the Pareto front approximation, which have been obtained with WASF-GA. For each of these individuals, the algorithm checks if it satisfies the constraints, and therefore, it is in the feasible set S. Then, among all those feasible points satisfying the constraints, the one with the lowest value for a minimization problem (or the higher value for a maximization problem) is selected.

Algorithm 2 Decision Tool (f, S, $\{\mathbf{x}_1, \mathbf{x}_2, \ldots, \mathbf{x}_N\}$)

Set $f_{\min} = 10^9$
for $j = 1, \ldots, N$
    if $\mathbf{x}_j \in S$
        Calculate $f(\mathbf{x}_j)$
        if $f(\mathbf{x}_j) < f_{\min}$
            $f_{\min} = f(\mathbf{x}_j)$
            $\mathbf{x}_{\min} = \mathbf{x}_j$
return $\mathbf{x}_{\min}$

3.5. The Multi–Layer Secant Genetic Algorithm

As introduced previously, for solving Problem (6), we can reformulate the multi-objective problem as a constrained mono-objective optimization problem of the form (5). To solve this new problem, we propose using the mono-objective algorithm MLS-GA explained below.

The mono–objective optimization algorithm considered here, denoted by MLS-GA, is a combination of three methods: a multi–layer line search algorithm (ML) [22], a mono-objective genetic algorithm (GA) and a Steepest Descent algorithm (SD) (see [23]). From a general point of view, the ML intends to provide a good initial population for the considered GA to speed up its convergence and improve its precision. Then, the GA performs a coarse global search of the solution local optimum. Finally, the SD improves the accuracy of the solutions returned by the GA.

A general scheme of MLS-GA is shown in Algorithm 3. Notice that the following input parameters must be provided: the number $l_{\max}$ of layers for the ML, the number N_p of individuals in the GA population, the number N_g of GA generations, the crossover p_c and mutation p_m probabilities, the number N_{SD} of iterations for the SD, the initial descent step size ν_0, the number N_ν of iterations for the dichotomy methods used to determine the descent step size, and ϵ_{SD} the step size of the first order forward approximation of the gradient.

At the beginning of the MLS-GA, a first initial population, P_1^0, of N_p individuals is randomly generated using a uniform distribution. At each ML generation l, with $l = 1, \ldots, l_{\max}$, the GA is executed starting from the initial population P_l^0, during N_g generations and with crossover and mutation probabilities of p_c and p_m, respectively. At the end of the ML iteration a new initial population for the GA, P_{l+1}^0, is calculated by considering a secant method between each element in P_l^0 and the optimal individual returned by the GA, denoted by $\mathbf{x}_l$. We note that $\mathbf{x}_l$ is also introduced in P_{l+1}^0 by randomly replacing one individual of this population. After $l_{\max}$ iterations, the ML algorithm returns a solution $\mathbf{x}_{l_{\max}}$. Finally, this solution is improved by performing N_{SD} iterations of the SD. The descent step size is determined using N_ν iterations of a dichotomy method starting from ν_0. The gradient is approximated by a first order forward approximation of step size ϵ_{SD}.

A detailed description of this algorithm MLS-GA, including the sub-processes (selection, crossover, mutation and elitism) used by the GA, can be found in [22].

4. Numerical Experiments

In this section, we outline the numerical experiments used to validate our multi-objective optimization approach. Firstly, we present the numerical implementation of the HPT model and its parameters. Secondly, we propose a multi-objective optimization problem and give the parameters of the WASF-GA used to solve it. Finally, we describe some constrained mono-objective optimization problems and the parameters of MLS-GA used to find their solutions.

Algorithm 3 MLS-GA ($l_{\max}$, f, N_p, N_g, p_c, p_m, N_{SD}, ν_0, N_ν, ϵ_{SD})

Set $l = 1$, $P_1^0 =$ initial population of N_p randomly generated individuals
while $l < l_{\max}$
  Calculate $\mathbf{x}_l = \mathrm{GA}(P_l^0, N_p, N_g, p_c, p_m)$ ▷ *Running Genetic Algorithm*
  for $j = 1, \ldots, N_p$
    ▷ *Construction of the next initial population* $P_{l+1}^0 = \{\mathbf{x}_{l+1,1}^0, \ldots, \mathbf{x}_{l+1,N_p}^0\}$
    if $f(\mathbf{x}_l) = f(\mathbf{x}_{l,j}^0)$
      $\mathbf{x}_{l+1,j}^0 = \mathbf{x}_{l,j}^0$
    else
      $\mathbf{x}_{l+1,j}^0 = \mathrm{proj}_S\left(\mathbf{x}_{l,j}^0 - f(\mathbf{x}_l)\frac{\mathbf{x}_l - \mathbf{x}_{l,j}^0}{f(\mathbf{x}_l) - f(\mathbf{x}_{l,j}^0)}\right)$
  $l = l + 1$
Calculate $\mathbf{x}_o = \mathrm{SD}(\mathbf{x}_{l_{\max}}, N_{SD}, \nu_0, N_\nu, \epsilon_{SD})$
return $\mathbf{x}_o$

We note that all the computations done during this work have been performed on a 7–Core processor with 3.6 GHz and 32Gb of RAM.

4.1. HPT process numerical implementation and parameters

For the numerical experiments performed during this work, we have considered a cylindrical steel high–pressure vessel similar to the pilot unit (ACB GEC Alsthom, Nantes, France) that was described in [13, 11]. It has a 0.09 m radius and a 0.654 m height corresponding to L and H in Figure 1, respectively. The pressurizing fluid chamber has a 0.05 m radius and a 0.25 m height, while the packed food domain has a 0.045 m radius and a 0.18 m height. The cap of the sample holder has the same radius but a 0.04 m height. We have set $H_1 = H_2 = 0.222$ m. Therefore, according to Figure 1, $H_3 = 0.402$ m, $H_4 = 0.442$ m, and $H_5 = 0.472$ m; $L_1 = 0.045$ m and $L_2 = 0.05$ m.

The numerical simulations for solving System (1) were done using the software COMSOL Multiphysics 5.0 based on the Finite Element Method (FEM) [24]. Temperature spatial discretization was based on P2 Lagrange Finite Elements. The time integration was performed considering the Backward Differentiation Formula method implemented on this platform. The nonlinear systems were solved with a damped Newton method and the algebraic linear systems were solved applying the MUMPS (MUltifrontal Massively Parallel sparse direct Solver).

For the convective heat transfer boundary, the ambient temperature and the heat transfer coefficient were set to $T_{\mathrm{amb}} = 19.3$ °C and $h = 28$ W m^{-2}K^{-1}, respectively. The thermophysical properties of the steel and the rubber cap of the sample holder were assumed to be constant (see [11]) and are reported on Table 1. Additionally, we considered liquid water as the pressurizing medium and tylose as the solid food sample. Indeed, tylose is a methyl cellulose gel whose thermophysical characteristics are similar to meat [25]. In order to take into account the dependence on temperature and pressure of water and tylose, their thermophysical properties were estimated using the shifting approach [26].

First, for water, the coefficients ρ, C_p and k were calculated at atmospheric conditions by the corresponding equations obtained by linear regression from data. Then, they were evaluated at high pressure by shifting the previous properties at atmospheric pressure. In the case of tylose, ρ, C_p and k were obtained by a rescaling procedure from the ones of water [27, 25] assuming that the ratio of these properties of water and tylose at ambient pressure is preserved at elevated pressures. In both cases, for the parameter α we used the expression described in [28].

Table 1: Thermophysical properties of the materials.

	Steel (Ω_{F})	Rubber (Ω_{C})
ρ ($\mathrm{Kg\,m^{-3}}$)	7833	1110
C_p ($\mathrm{J\,Kg^{-1}K}$)	465	1884
k ($\mathrm{W\,m^{-1}K^{-1}}$)	55	0.173

Additionally, we considered a processing time of $t_f = 900$ seconds. We note that the initial temperature T_0, the refrigeration temperature T_{r} and the equipment pressure P varying in time t, are the parameters of the optimization problems introduced later in Sections 4.2 and 4.3.

In our work, we have considered the enzyme called *Bacillus Subtilis* α–*Amylase* (BSAA) produced by a bacteria present in the ground and which can contaminate food and modify its taste [17], and the vitamin C, that is present in some fruits and which has good antioxidant properties [29]. The inactivation rates of this particular enzyme and vitamin are calculated using Equation (2) with the parameters presented on Table 2 which have been reported in [17] and [29], respectively.

Table 2: Inactivation rate parameters.

	BSAA	Vitamin C
T_{ref} (K)	313	373
P_{ref} (MPa)	500	700
κ_{ref} ($\mathrm{min^{-1}}$)	3.9e-2	$4 \times$ 1.98e-2
B (K)	10097	9071.4
C ($\mathrm{MPa^{-1}}$)	-8.7e-4	-0.00555

With the aim of solving Equation (3) numerically, the time interval $[0, t_f]$ is discretized as $0 = t_0 < t_1 < \cdots < t_n = t_f$ with a fixed step $\tau = t_i - t_{i-1} = \frac{t_f}{n}$, for $i = 1, 2, \ldots, n$. The enzymatic activity is evaluated on an equally distributed mesh in the food sample domain Ω_{F}. Given $(r, z) \in \Omega_{\mathrm{F}}$ and denoting $\kappa_j(r, z) = \kappa\big(P(t_j), T(r, z, t_j)\big)$, a numerical approximation of the function defined in (4)

can be obtained considering the trapezoidal formula

$$A(r,z,t_n) \approx A(r,z,0)\exp\left(-\frac{\tau}{2}\sum_{j=0}^{n-1}\Big(\kappa_j(r,z)+\kappa_{j+1}(r,z)\Big)\right). \tag{8}$$

4.2. Considered multi–objective optimization problem and settings

The case under study aims to optimize the HPT process, in the sense that the activity of the enzyme BSAA and the maximum temperature during the whole process are minimized, and the activity of the Vitamin C is maximized, at the same time. Therefore, this problem is formulated as a multi-objective problem as follows:

$$\begin{cases} \min & f_{\text{bsaa}}(T_0,T_r,P), \\ \max & f_{\text{vit}}(T_0,T_r,P), \\ \min & f_{\text{Tmax}}(T_0,T_r,P), \end{cases} \tag{9}$$

where the decision variables are the initial, T_0, and refrigeration, T_r, temperatures and a piece-wise linear function P (depending on time), defining the equipment pressure evolution. Additionally, those decision variables are constrained due to the equipment restrictions detailed below (e.g., temperature and pressure admissible range).

The numerical solution of System (1) is used to obtain the final activity values of enzyme and vitamin and the maximum temperature under the HPT process described by the decision variables. More precisely, we consider:

$$f_{\text{bsaa}}(T_0,T_r,P) = \frac{1}{|\Omega_{\text{F}}|}\iint_{\Omega_{\text{F}}} A_{\text{bsaa}}(r,z,t_f)drdz,$$

$$f_{\text{vit}}(T_0,T_r,P) = \frac{1}{|\Omega_{\text{F}}|}\iint_{\Omega_{\text{F}}} A_{\text{vit}}(r,z,t_f)drdz.$$

Those functions correspond to the average activity in the food sample domain of the enzyme and vitamin, respectively.

The third objective function f_{Tmax}, which computes the maximum temperature reached in the food sample along the whole HPT treatment, can be expressed by:

$$f_{\text{Tmax}}(T_0,T_r,P) = \max_{(r,z)\in\Omega_{\text{F}},\ t\in[t_0,t_f]} T(r,z,t).$$

In order to design the pressure evolution function P, we consider an initial equipment pressure $P_0 = 0.1$ (MPa) (i.e., atmospheric pressure) at time $t_0 = 0$ seconds. Then, we consider $n+1$ time intervals $[t_i, t_{i+1}]$, with $t_i = i \cdot \frac{900}{n}$, $i \in \{1,\cdots,n\}$, and, at each interval, we consider a constant pressure variation $\Delta P_i \in [\Delta P_{n,\text{dec}}, \Delta P_{n,\text{inc}}]$ (MPa), where $\Delta P_{n,\text{dec}}$ and $\Delta P_{n,\text{inc}}$ are the maximum variations allowed by the equipment for the decrease and for the increase in pressure, respectively, during $900/n$ seconds. However, those pressure variations cannot generate pressure out of the equipment admissible pressure range

$[P_{\min}, P_{\max}]$ (MPa). Finally after 900 seconds, the pressure is decreased at a constant fixed rate of $\Delta P_{n,\text{dec}} \cdot (n/900)$ (MPa$\cdot$s^{-1}) up to reaching 0.1 MPa. Thus, $P(t)$ is built by considering the linear interpolation through the points $\{(i * 900/n \text{ (s)}, P_i \text{ (MPa) })\}_{i=0}^{n} \cup \{(900 + (P_n - 0.1)/|\Delta P_{n,\text{dec}}| \text{ (s)}, 0.1 \text{ (MPa) })\}$, with $P_i = P_{i-1} + \Delta P_i$ for $i \in \{1, \cdots, n\}$.

In this work, taking into account the restriction of the considered pressure vessel, we consider that the range of admissible temperature is [10, 50] (°C), the range of admissible pressure is [0.1, 900] (MPa) and the range of admissible variations for the pressure is $[\Delta P_{n,\text{dec}}, \Delta P_{n,\text{inc}}] = [-250, 250]$ (MPa).

Thus, the discrete version of Problem (9) considered here is:

Problem 1.

$$\begin{cases} \min & f_{\text{bsaa}}(T_0, T_r, \Delta P_1, \ldots, \Delta P_n), \\ \max & f_{\text{vit}}(T_0, T_r, \Delta P_1, \ldots, \Delta P_n), \\ \min & f_{\text{Tmax}}(T_0, T_r, \Delta P_1, \ldots, \Delta P_n). \\ \text{s.t.} & T_0, T_r \in [10, 50](^\circ\text{C}) \\ & \Delta P_1, \ldots, \Delta P_n \in [-250, 250](\text{MPa}) \end{cases} \tag{10}$$

The implementation of WASF-GA provided by the framework jMetal [30] has been used. jMetal is an object-oriented Java-based framework aimed at the development, experimentation, and study of metaheuristics for solving multi-objective optimization problems. For our numerical experiments, jMetal has been connected with the COMSOL solver, which carries out the simulation of the HPT process and returns the values of the objective functions.

The considered preferences of the DM when solving this problem were: (i) There cannot be enzymatic activity, (ii) all the vitamin activity must be maintained and (iii) the final maximum temperature must be 30°C. Such information has been included in WASF-GA through the reference point $(0.0, 0.0, 30.0)$.

The behavior of WASF-GA, in terms of efficiency and effectiveness, depends largely on the input parameters. For the case at hand, the parameter η has been fixed to 0.001, as stated in [10]. Similarly, the sample of weight vectors $\{\mu^1, \ldots, \mu^{N_\mu}\}$ has been computed by setting $N_\mu = N$, and following the procedure explained in [10]. The remaining input parameters, i.e., the number N of individuals in the population and the number of generations $h_{\max}$ of the optimization procedure, have been analyzed looking for an equilibrium between quality of the solution and computational cost. Table 3 summarizes the values studied for these two parameters. For the sake of completeness, the number of function evaluation *eval* consumed when N and $h_{\max}$ are considered has also been included. Notice that $eval = N \cdot h_{\max}$.

Table 3: Considered values of N and $h_{\max}$ for the performance study of WASF-GA.

N	50	100	200	300
$h_{\max}$	20	30	33	36
eval	1000	3000	6600	10800

Additionally, in order to accomplish a comprehensive analysis, the parameters that influence the crossover and the mutation have also been studied. In particular, four different settings have been considered which have been named with letters from A to D. Table 4 shows the considered values for the probability and distribution of both crossover and mutation. Notice that setting A coincides with the proposed values in [10].

Table 4: Probability and distribution values of crossover and mutation considered for the performance study of WASF-GA.

		A	B	C	D
Crossover	Probability	0.9	0.9	0.5	0.9
	Distribution	20.0	20.0	20.0	10.0
Mutation	Probability	0.1	0.5	0.1	0.1
	Distribution	20.0	20.0	20.0	10.0

Hence, for the input parameter study, for each number of *eval* on Table 3, the four settings on Table 4 have been considered, making a total of $l_{\max} = 16$ combinations. Furthermore, due to the stochastic nature of the algorithm, for each setting l, $l \in \{1, \ldots, l_{\max}\}$, $rs_l = 10$ runs are performed, generating the approximation sets $PS_1^l, \ldots, PS_{rs_l}^l$ (in the decision space). Lets denote by SPS the set of all the approximation sets of the Pareto set, $SPS = \{PS_1^1, \ldots, PS_{rs_1}^1, \ldots, PS_1^{l_{\max}}, \ldots, PS_{rs_{l_{\max}}}^{l_{\max}}\}$.

An important question now is how to analyze the performance of WASF-GA with each setting l. Notice, that from an engineering point of view, it is not as interesting to obtain the most accurate approximation to the real Pareto front, but to achieve a good enough approximation in a reasonable computing time. To research this, some descriptive measurements are needed.

The efficiency of WASF-GA will be measured through the computing time, in particular, the average time Av(Time) of the 10 runs will be computed.

The effectiveness will be researched by analyzing (i) how many different constrained mono-objective problems have been solved and (ii) their closeness to the global optima. In this sense, notice that the better distributed the approximation set is (in the decision space), the larger the number of different mono-objective problems have been solved. Additionally, the closer the approximation set to the real Pareto-front, the better the quality of the solutions provided. The well-known *hypervolume* is able to measure both circumstances in a single figure. In fact, it can be thought of as a global quality indicator, in the sense that it assesses the approximation set as a whole [31, 32]. In the following, some details about how this metric has been computed here, are provided.

4.2.1. Hypervolume quality indicator

This Pareto compliant indicator measures the hypervolume of the portion of the criterion space that is weakly dominated by the approximation set. The

Algorithm 4 Computation of Hypervolume indicator

1: Compute nadir point $\mathbf{z}^{\text{nad}} = (f_1^{(\max)}, f_2^{(\max)})$
2: Set $hyper = 0$
3: **for** $ic = 1$ to $(L_{\max} - 1)$
4: $\quad hyper = hyper + (f_2^{(\max)} - f_2^{(ic)}) \cdot (f_1^{(ic+1)} - f_1^{(ic)})$
5: $hyper = hyper + (f_2^{(\max)} - f_2^{(L_{\max})}) \cdot (f_1^{(\max)} - f_1^{(L_{\max})})$

higher the hypervolume, the better the approximation.

In order to measure this quantity, an approximation of the nadir point, which is dominated by all points, is needed. It has to be the same approximate nadir point for all the runs and all the configurations to allow a fair comparison. In the presented computational studies, the point whose i-th component is the maximum of all the i-th components of points in $f(SPS)$ is considered as an approximation of the Nadir point obtained when considering all the approximations of the Pareto-front together.

In Algorithm 4, a description of how to compute the hypervolume when two objective functions are considered, f_1 and f_2, is given. The first step is to compute this approximate nadir point $\mathbf{z}^{\text{nad}} = (f_1^{(\max)}, f_2^{(\max)})$, where $f_i^{(\max)}$ denotes the maximum value of f_i with $i = 1, 2$ when considering all the solutions in SPS. Then, the hypervolume is calculated as the area covered by the points of the Pareto-front and the considered nadir point $\mathbf{z}^{\text{nad}}$. In Figure 3 a graphic representation of this metric is given for a bi-objective optimization problem. In particular, the figure on the left hand shows the calculation procedure of the hypervolume metric and the figure on the right illustrates how the hypervolume increases as the number of points in the Pareto-front does.

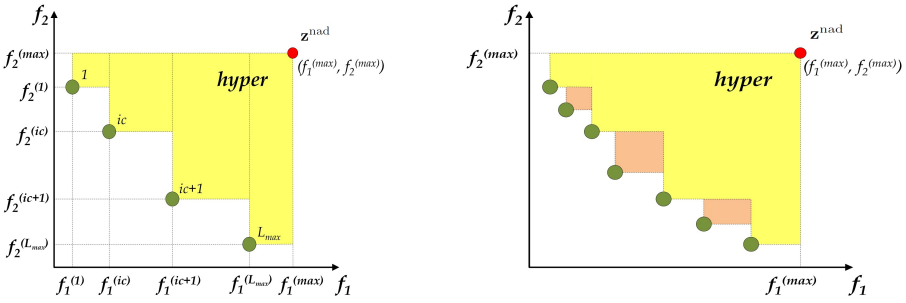

Figure 3: Hypervolume ($hyper$) calculation.

For computing the hypervolume, the objective values are previously normalized such that they contribute equally to the measure indicator. The following

standard normalization is used:

$$f_i(\mathbf{x})' = \frac{f_i(\mathbf{x}) - f_i^{(\min)}}{f_i^{(\max)} - f_i^{(\min)}},$$

where $f_i^{(\min)}$ (resp. $f_i^{(\max)}$) denotes the minimum (resp. maximum) value of f_i when considering all the solutions in SPS.

4.3. Considered mono–objective optimization problems and settings

In some particular cases, the DM could consider solving constrained mono-objective problems according to some specific quality requirements (e.g., organoleptic properties).

For instance, the DM could be interested in obtaining the optimal HPT configuration which minimizes the final enzymatic activity maintaining the vitamin activity above 97% (denoted as **Problem 2**) or maximize the vitamin keeping the enzyme activity below 40% (denoted as **Problem 3**). In both cases, a temperature constraint is assumed so that it does not surpass a pre-determined upper limit. Both of those particular cases can be reformulated as:

Problem 2.

$$\begin{array}{ll} \min & f_{\text{bsaa}}(T_0, T_r, \Delta P_1, \ldots, \Delta P_n), \\ \text{s.t.} & f_{\text{vit}}(T_0, T_r, \Delta P_1, \ldots, \Delta P_n) \geq 0.97, \\ & f_{\text{Tmax}}(T_0, T_r, \Delta P_1, \ldots, \Delta P_n) \leq 50, \\ & T_0, T_r \in [10, 50](^\circ\text{C}), \\ & \Delta P_1, \ldots, \Delta P_n \in [-250, 250](\text{MPa}), \end{array} \tag{11}$$

which is approximated by the following penalty problem:

$$\begin{array}{ll} \min & \Big[f_{\text{bsaa}} + 10^9 \max\{0.97 - f_{\text{vit}}, 0.0\} + 10^9 \max\{f_{\text{Tmax}} - 50, 0.0\} \Big], \\ \text{s.t.} & T_0, T_r \in [10, 50](^\circ\text{C}), \\ & \Delta P_1, \ldots, \Delta P_n \in [-250, 250](\text{MPa}). \end{array} \tag{12}$$

Problem 3.

$$\begin{array}{ll} \max & f_{\text{vit}}(T_0, T_r, \Delta P_1, \ldots, \Delta P_n), \\ \text{s.t.} & f_{\text{bsaa}}(T_0, T_r, \Delta P_1, \ldots, \Delta P_n) \leq 0.4, \\ & f_{\text{Tmax}}(T_0, T_r, \Delta P_1, \ldots, \Delta P_n) \leq 47, \\ & T_0, T_r \in [10, 50](^\circ\text{C}), \\ & \Delta P_1, \ldots, \Delta P_n \in [-250, 250](\text{MPa}), \end{array} \tag{13}$$

which is approximated by the following penalty problem:

$$\begin{array}{ll} \max & \Big[f_{\text{vit}} - 10^9 \max\{f_{\text{bsaa}} - 0.4, 0.0\} - 10^9 \max\{f_{\text{Tmax}} - 47, 0.0\} \Big], \\ \text{s.t.} & T_0, T_r \in [10, 50](^\circ\text{C}), \\ & \Delta P_1, \ldots, \Delta P_n \in [-250, 250](\text{MPa}). \end{array} \tag{14}$$

Problem 2 and **Problem 3** have been solved with the MLS-GA described in Section 3.5 using the Matlab implementation included in *Global Optimization Platform* GOP (available at: `http://www.mat.ucm.es/momat/software.htm`), an open access Matlab optimization toolbox which has already been successfully used in many industrial problems [33, 34, 35, 36, 37, 38]. This platform has been coupled with COMSOL Multiphysics 5.0 in order to evaluate the objective function.

As done for the multi-objective methodology presented previously, the behavior of the MLS-GA has also been studied for different population sizes by performing 10 independent runs for each case. In particular, three population sizes for the GA method has been considered: $N_p = 40$, $N_p = 100$ and $N_p = 180$ (see Table 5).

The remaining parameter settings for the MLS-GA are the following:

- Regarding the GA method, the number of generations has been set to $N_g = 30$, and probabilities of $p_c = 0.45$ and $p_m = 0.5$ have been considered, respectively, for crossover and mutation. These parameter values have been chosen because they provide good results on other complex optimization problems [39, 40].

- For the MLS, $l_{\max} = 5$ iterations of internal layer have been used (i.e., we run the GA 5 times starting from an improved initial population).

- At the end, $N_{SD} = 10$ iterations of the SD, using a first order Taylor approximation of the gradient with 5% (i.e., $\epsilon_{SD} = 0.05$) perturbation in each variable, have been carried out. The initial descent step size is $\nu_0 = 0.1$ and the number of iterations used for determining the step size is $N_\nu = 5$.

The total number of evaluations of the MLS-GA, without taking into account the SD evaluations, is given by $eval = N_p \cdot N_g \cdot l_{\max}$ (see Table 5).

Table 5: Values of N_p, N_g and $l_{\max}$ for the performance study of the MLS-GA.

N_p	40	100	180
N_g	30	30	30
$l_{\max}$	5	5	5
$eval$	6000	15000	27000

5. Results and discussion

This section is devoted to studying and validating the interest that food engineers have in using a Pareto set approximation (and its corresponding Pareto front approximation) as a decision tool. In particular, we study if the solutions of the approximate Pareto front are adequate to solve constrained mono-objective problems by comparing the solutions provided by WASF-GA and by MLS-GA.

To this aim, in Section 5.1, the behavior of the WASF-GA is analyzed for different settings of parameters. In Section 5.2, the performances of the MLS-GA for solving those mono-objective problems are also analyzed. Then, in Section 5.3, we compare the solutions obtained with both methodologies. Additionally, for the WASF-GA algorithm, the optimal HPT configurations of each of the mono-objective problems are discussed in Section 5.4, including a sensitivity analysis regarding the decision parameters. Finally, in Section 5.5, those optimal solutions are improved by using an additional layer of an SD method as a local optimizer.

5.1. Results obtained with the WASF-GA

In this subsection, the performances of WASF-GA for approximating Pareto-fronts have been analyzed for the 16 sets of parameters proposed in Section 4.2. To do so, for each parameter configuration, we have first approximated the Pareto front associated to **Problem 1**. Then, considering **Problem 2** and **Problem 3**, we have extracted the solutions of the generated Pareto front that better solve both of those mono-objective problems. Each experiment has been repeated 10 times.

For the sake of simplicity, we only report the most relevant results obtained in those experiments on Table 6. More precisely, for each setting, the following values are shown: (i) the minimum (denoted by $\text{Min}(f_{\text{bsaa}})$), the average ($\text{Av}(f_{\text{bsaa}})$) and the maximum ($\text{Max}(f_{\text{bsaa}})$) value of the enzymatic activity (in %); (ii) the minimum ($\text{Min}(f_{\text{vit}})$), the average ($\text{Av}(f_{\text{vit}})$) and the maximum ($\text{Max}(f_{\text{vit}})$) value of the vitamin activity (in %); (iii) the mean hypervolume value (Av(HV)), described in Subsection 4.2.1, and the average computing time (Av(Time)) in hours.

Table 6: Results obtained by using the Pareto front of **Problem 1** computed with WASF-GA for solving **Problem 2** and **Problem 3**: minimum (Min), average (Av) and maximum (Max) values of the final enzymatic activity f_{bsaa} (resp. vitamin activity f_{vit}), which is the objective function to minimize (resp. maximize) in **Problem 2** (resp. **Problem 3**). The last two columns report the averages of hypervolume (HV) and computing time (Time) in hours, respectively.

		Selected solution for **Problem 2**			Selected solution for **Problem 3**				
Eval.		Min(f_{bsaa})	Av(f_{bsaa})	Max(f_{bsaa})	Min(f_{vit})	Av(f_{vit})	Max(f_{vit})	Av(HV)	Av(Time)
1000	A	0.286	0.324	0.364	-	-	-	0.5135	5.17
	B	0.293	0.333	0.377	-	-	-	0.5132	5.33
	C	0.282	0.352	0.395	-	-	-	0.5009	5.18
	D	0.306	0.331	0.352	-	-	-	0.5100	5.16
3000	A	0.258	0.281	0.306	-	-	-	0.5608	15.10
	B	0.281	0.290	0.306	-	-	-	0.5442	15.79
	C	0.265	0.292	0.309	-	-	-	0.5491	14.47
	D	0.281	0.288	0.296	-	-	-	0.5606	14.44
6600	A	0.245	0.256	0.269	0.977	0.990	0.996	0.5629	34.58
	B	0.271	0.279	0.285	0.984	0.991	0.995	0.5586	34.62
	C	0.263	0.277	0.301	0.990	0.994	0.992	0.5514	34.50
	D	0.257	0.261	0.265	0.994	0.996	0.995	0.5604	34.27
10800	A	0.251	0.255	0.259	0.988	0.991	0.994	0.5725	54.15
	B	0.258	0.262	0.267	0.993	0.994	0.995	0.5611	55.48
	C	0.246	0.253	0.260	0.989	0.991	0.993	0.5625	55.00
	D	0.257	0.259	0.261	0.995	0.995	0.995	0.5714	55.17

Focusing on the multi-objective problem, according to the hypervolume

value, the most adapted setting for the crossover and mutation parameters seems to be the configuration A. Bear in mind that the larger the hypervolume is, the better the approximation of the Pareto front is. The execution time seems to be similar independently of the choice of setting.

Now, we analyze the results obtained by the WASF-GA for the mono-objective problems **Problem 2** and **Problem 3**. We note that for **Problem 3** some values have been omitted. Indeed, for the corresponding settings, in one or more runs it occurs that no solution in the Pareto set approximation satisfies the constraint on the enzymatic activity. In fact, in order to obtain feasible solutions to Problem 3, a number of 6600 function evaluations of the WASF-GA seems to be needed, reagardless the setting A, B, C or D. As can be seen on Table 6, the larger the number of function evaluations is, the better the effectiveness of WASF-GA for obtaining an approximate solution of a mono-objective constrained problem is, but the longer the computing time will be. For example, lets consider the setting parameter A, the hypervolume increases from 0.5135 with 6600 to 0.5725 with 10800 function evaluations. In the same way, the computing time also increases from 34.58 to 54.15 hours.

5.2. Results obtained with the MLS-GA

Now, we analyze the behavior of the MLS-GA for solving the mono-objective problems **Problem 2** and **Problem 3**.

To this aim, the MLS-GA was executed with three different sets of parameters when dealing with those problems (see Subsection 4.3 and Table 5). Again, each particular case was solved 10 times, and hence, average values are provided. Table 7 and Table 8 summarize the obtained results. In particular, the minimum, the average and the maximum values of the final enzymatic (resp. vitamin) activity, which is the objective function to minimize (resp. maximize) for **Problem 2** (resp. **Problem 3**), are reported. Additionally, the average computing time (in hours) is also shown. Notice that for **Problem 3** and 6000 evaluations, the corresponding values for the vitamin activity have not been included because no solution in any run satisfies the enzymatic activity constraint.

We recall that **Problem 2** is a minimization problem whereas **Problem 3** is a maximization one. In all cases, we observe that the effectiveness of the MLS-GA improves as the number of function evaluations increases. Regarding the computational time, it increases almost linearly with the number of function evaluations. For instance, the MLS-GA with 27000 evaluations, it takes around 93.65 hours to provide a solution, which is not a negligible value.

Table 7: Solutions to **Problem 2** obtained by the MLS-GA for different parameter settings: minimum (Min), average (Av) and maximum (Max) values of the final enzymatic activity f_{bsaa}. The last column reports the average computing time Av(Time) in hours.

Eval.	Min(f_{bsaa})	Av(f_{bsaa})	Max(f_{bsaa})	Av(Time)
6000	0.293	0.304	0.315	25.33
15000	0.279	0.282	0.284	48.40
27000	0.252	0.262	0.268	117.58

Table 8: Solutions to **Problem 3** obtained by the MLS-GA for different parameter settings: minimum (Min), average (Av) and maximum (Max) values of the final vitamin activity f_{vit}. The last column reports the average computing time Av(Time) in hours.

Eval.	Min(f_{vit})	Av(f_{vit})	Max(f_{vit})	Av(Time)
6000	-	-	-	24.94
15000	0.976	0.983	0.995	45.03
27000	0.978	0.988	0.993	93.65

5.3. Comparison between the WASF-GA and the MLS-GA results

In this subsection, in order to show the interest of the proposed methodology in solving mono-objective problems, the WASF-GA and the MLS-GA results have been compared for both **Problem 2** and **Problem 3**.

The first comparison has been made by using settings with similar computing time. More precisely, the results returned by the WASF-GA with 6600 evaluations and the four different setting configurations (A, B, C and D) have been compared to the MLS-GA ones with 15000 evaluations. These results are shown on Table 6 for the WASF-GA and Tables 7 and 8 for the MLS-GA.

Contrasting them, it can be observed that, for **Problem 2**, the minimum Min(f_{bsaa}) and the average Av(f_{bsaa}) values of the objective function obtained by the WASF-GA with all the settings are lower than the ones returned by the MLS-GA. As we are interested in minimizing function f_{bsaa}, we deduce that the WASF-GA seems to provide better results than MLS-GA (i.e., lower values of f_{bsaa}). Regarding the value of Max(f_{bsaa}), the WASF-GA also overcomes the MLS-GA for the settings A and D by achieving lower values. Moreover, we observe that, for setting A and D, the values of Max(f_{bsaa}) on Table 6 (i.e., 0.269 and 0.265, respectively) are lower than the value Min(f_{bsaa}) obtained by the best solution returned by the MLS-GA solution (i.e., 0.279, see Table 7). Therefore, even in the worst cases, the solutions given by the WASF-GA with an adequate set of parameters seem to be better than the solutions found with the MLS-GA.

Tackling **Problem 3**, as the objective is to maximize the vitamin activity, the larger the objective function value is, the better the solution is. Again, the WASF-GA exhibits better results for settings A to D (i.e., greater minimum

and average values of f_{vit}) than the MLS-GA. We observe that the maximum vitamin activities (i.e., Max(f_{vit})) of the solutions returned with the WASF-GA, with setting A, B and D, are similar to the values found by the MLS-GA. Notice that, for **Problem 3**, the lowest values of Min(f_{vit}) of the solutions given by the WASF-GA with settings B, C and D are higher than the average value Av(f_{vit}) of the MLS-GA one. For this particular example, it seems that the WASF-GA also returns better solutions than the MLS-GA.

Secondly, we compare the results obtained with the most computational extensive set of parameters of both algorithms that is: the WASF-GA employing 10800 function evaluations and the MLSA-GA with 27000 function evaluations. In this case, the computing time of the MLS-GA is, as expected, almost twice longer than the execution time of the WASF-GA.

On the one hand, for **Problem 2**, the WASF-GA with settings A and C returns minimum values of the enzymatic activity (i.e., 0.251 and 0.246, respectively, see Min(f_{bsaa}) on Table 6) lower, and consequently better, than the MLS-GA minimum value (i.e., 0.252 see Table 7). The WASF-GA average values (i.e., Av(f_{bsaa}) with sets A, C or D are also better than the MLS-GA average value. In the case of setting B, both algorithms provide similar average values. Regarding the values Max(f_{bsaa}), the WASF-GA ones are always better (i.e., lower) than the MLS-GA one. Although they are the worst WASF-GA results for the enzymatic activity, those WASF-GA maximum values for the sets A, C or D are even lower than the MLS-GA average value.

On the other hand, for **Problem 3**, the minimum and the average values of f_{vit} obtained by the WASF-GA are always better (i.e., greater) than the ones achieved by the MLS-GA. Additionally, the maximum values provided by the WASF-GA are also greater than the MLS-GA one for all the settings, except for C for which they are similar. Notice that, for **Problem 3**, the worst WASF-GA values corresponding to Min(f_{vit}) are better or equal than the average value Av(f_{vit}) of the MLS-GA.

Those results seem to indicate that the results obtained with the WASF-GA with 10800 function evaluations have better characteristics than those returned by the MLSA-GA with 27000 function evaluations.

Finally, we compare the efficiency of the WASF-GA using 6600 evaluations and the MLS-GA with 27000 evaluations.

Although the WASF-GA exhibits the lowest computing time, for **Problem 2** it can be observed that:

- The minimum value (Min(f_{bsaa})) found among the results of the different WASF-GA runs with the setting A is lower than the minimum found among the different MLS-GA solutions.
- The WASF-GA average value (Av(f_{bsaa})) using the settings A and D is lower than the MLS-GA average.
- The WASF-GA maximum value (Max(f_{bsaa})) considering the setting D is also lower than the MLS-GA maximum value.

Therefore, the WASF-GA configured with the parameters A and D has results that are similar, or even better, than those obtained with the MLS-GA, despite the fact that the WASF-GA consumes less computational time.

For **Problem 3**, it seems that the WASF-GA also overcomes the MLS-GA. Indeed, we notice that:

- The WASF-GA minimum values ($\mathrm{Min}(f_{\mathrm{vit}})$) for settings B, C and D are higher than the MLS-GA minimum. In particular, for setting B, this value is higher than the MLS-GA average one. Finally, for setting D, this value is higher than the MLS-GA maximum, which means that the worst WASF-GA case is better than the best MLS-GA solution.

- The WASF-GA average value ($\mathrm{Av}(f_{\mathrm{vit}})$) is higher and, consequently, better than the MLS-GA average value for all the settings.

- The WASF-GA maximum ($\mathrm{Max}(f_{\mathrm{vit}})$) is also higher than the MLS-GA maximum for all the settings, except C.

On Table 9, we summarize the results obtained when comparing the WASF-GA and the MLS-GA detailed above. On this table, we have labelled with "+" when the WASF-GA value is better than the MLS-GA one, "=" when both algorithms exhibit similar values and "-" when the WASF-GA has worse values than the MLS-GA ones. Additionally, dark grey cells means that the worst WASF-GA solution overcomes the best MLS-GA one and soft grey cells are employed when the worst WASF-GA value is better than the average value returned by the MLS-GA. If both facts happen, dark grey cells are used.

We can observe on this table that, from a general point of view, the WASF-GA provides better solutions for both problems, even when the computational time of the WASF-GA is lower than the one of the MLS-GA. In particular, the WASF-GA with setting A and 10800 evaluations is the most suitable option. However, for the same setting A, the WASF-GA using 6600 evaluations is also a quite valuable option as it also achieves reasonable results with lower computational time.

Table 9: Comparison between WASF-GA and MLS-GA in terms of the minimum (Min), average (Av) and maximum (Max) values of the final enzymatic activity for **Problem 2** and the final vitamin activity for **Problem 3**. The average computing time in hours is also reported. We use "+", "=" and "-" when the WASF-GA value is better than, similar, or worse than the MLS-GA one, respectively. Dark grey means that the worst WASF-GA solution overcomes the best MLS-GA one and soft grey means that the worst WASF-GA value is better than the average value returned by the MLS-GA.

MLS-GA / WASF-GA		Eval.	15000						27000					
			Problem 2			**Problem 3**			**Problem 2**			**Problem 3**		
		Av(Time)	48.40			45.03			117.58			93.65		
			Min	Av	Max	Min	Av	Max	Min	Av	Max	Min	Av	Max
6600	A	34.54	+	+	+	+	+	+	+	+	-	-	+	+
	B	34.62	+	+	-	+	+	=	-	-	-	+	+	+
	C	34.50	+	+	-	+	+	-	-	-	-	+	+	-
	D	34.27	+	+	+	+	+	=	-	+	+	+	+	+
10800	A	54.15	+	+	+	+	+	-	+	+	+	+	+	+
	B	55.48	+	+	+	+	+	=	-	=	+	+	+	+
	C	55.00	+	+	+	+	+	-	+	+	+	+	+	=
	D	55.17	+	+	+	+	+	=	-	+	+	+	+	+

Summarizing the results discussed aforementioned, the proposed decision methodology based on the WASF-GA allows us to find a point in the Pareto front set which seems to be at least as efficient as the MLS-GA solution and, in some cases, it seems to be even better than this mono-objective solution. Moreover, our decision methodology implies considerable savings in computing time. Indeed, if we use a mono-objective algorithm, we need to carry out a new run each time we change the constraints. However, if we employ our multi-objective approach, we can solve different problems with the same outcome obtained in a single run of the WASF-GA.

Looking for a reasonable ratio between the quality of the solution and the computational time, it seems that running the WASF-GA with 6600 function evaluations and the set of parameters A shows reasonable results.

5.4. Optimal HPT configurations

Once the interest of the multi-objective methodology has been discussed, we now focus on analyzing the solutions of **Problem 2** and **Problem 3** returned by the WASF-GA from a food engineering point of view. In particular, according to the result presented in Section 5.3, we consider the case of 6600 function evaluations with the setting A. For this particular configuration, the best solutions are reported on Table 10. Additionally, in Figure 4 the evolution of temperature and pressure, averaged in the food domain, for those optimal HPT configurations are plotted.

Table 10: Optimal HPT configurations obtained with the proposed multi-objective methodology for **Problem 2** (first row) and for **Problem 3** (second row). In particular, the two first columns contain the optimal values for the initial (T_0) and refrigeration (T_r) temperatures (in $^\circ$C) and the remaining columns show the optimal pressure variations ($\Delta P_1, \ldots, \Delta P_8$) values (in MPa).

	T_0	T_r	ΔP_1	ΔP_2	ΔP_3	ΔP_4	ΔP_5	ΔP_6	ΔP_7	ΔP_8
P2	32.06	42.40	249.61	229.14	100.55	33.12	-4.28	1.16	0.82	-8.83
P3	32.64	42.41	244.12	197.37	5.49	11.33	-0.18	-4.68	5.52	-0.82

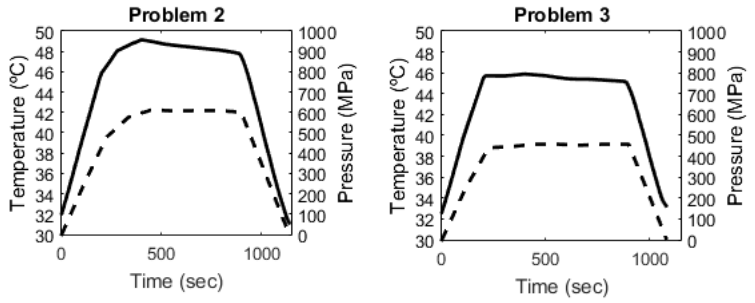

Figure 4: Evolution of temperature (continuous line) and pressure (dash line) averaged in the food domain of the optimal HPT configurations obtained with the proposed multi-objective methodology for **Problem 2** (top) and for **Problem 3** (bottom).

We can observe in Figure 4 that, in both cases, the pressure evolution is divided into three main parts: the first stage of pressure increase, the second one of almost constant pressure and, finally, the last stage of pressure decrease. From a practical point of view, those results seem to indicate that, for the considered cases, a continuous increase in the pressure up to reaching the constrained temperature and then maintaining the pressure constant is one of the most efficient strategies for treating the food sample. However, we note that the increase of the pressure is not constant and not equal to the maximum variation allowed by the equipment. This could be explained by the fact that a quick increase in the pressure provokes a rapid increment of the temperature and, thus, it could damage the vitamin. To illustrate this point, we have considered two cases where the pressure grows at a constant rate and then remains constant: the first one, calculating this constant growth rate by approximating linearly the optimal pressure profile found by the WASF-GA, and the second one, assuming a maximum variation rate per second of $\frac{250}{900/n}$ MPa·s^{-1} for the first step until reaching 500.1 MPa. In both cases, the obtained solutions are worse than the optimal solution provided by our methodology, mainly due to the fact that the maximum temperature constraint is not satisfied or they exhibit worse values of enzymatic or vitamin activities (see Table 11).

Table 11: Objective function values (f_{bsaa}, f_{vit}, f_{Tmax}) obtained for different HPT treatments: using the optimal configuration found by WASF-GA (first row), employing a constant growth rate (second row) and assuming a maximum variation rate of $\frac{250}{900/n}$ MPa·s^{-1} (third row).

	Problem 2			**Problem 3**		
	f_{bsaa}	f_{vit}	f_{Tmax}	f_{bsaa}	f_{vit}	f_{Tmax}
WASF-GA	0.2448	0.9882	49.85	0.3832	0.9957	46.57
Constant rate	0.2946	0.9935	49.09	0.3854	0.9957	47.30
Rate of $\frac{250}{900/n}$ MPa·s^{-1}	0.1939	0.9870	52.42	0.3298	0.9939	48.35

Finally, in order to determine the influence of each optimization parameter and analyze the robustness of the obtained solutions, we have carried out a sensitivity analysis. In particular, we have studied the impact on the BSAA final activity for **Problem 2**, and on the vitamin final activity for **Problem 3**, of perturbations on the decision parameters. To this aim, each parameter on Table 10 has been modified by $\pm\alpha\%$ of its value, respectively, where $\alpha = 1\%, 5\%, 10\%$, and 25%. Then, we have compared the enzymatic or vitamin activity obtained to the modified parameters, denoted by $\mathbf{x}_{\text{mod},i}$, with $i = 1, \ldots, 10$, to the optimized activities $\mathbf{x}_{\text{op}}$ by using a percent variation relation:

$$100\frac{|f_{\text{bsaa}}(\mathbf{x}_{\text{op}}) - f_{\text{bsaa}}(\mathbf{x}_{\text{mod},i})|}{f_{\text{bsaa}}(\mathbf{x}_{\text{op}})}.$$

On Table 12 and Table 13, we summarize the results of this study. As we can see, the initial and refrigeration temperatures seem to be the most influential parameters and the maximum percent variation in the enzymatic or vitamin final activity seems to grow linearly with the percent variation applied to each parameter. Those results seem to show that practitioners should intend to control perturbations in the temperatures that may occur during the implementation process. On the other hand, the solutions seem to be robust to reasonable variations in the pressure profile and, thus, imperfections of the pressure during the treatment should not have an impact on the general process performances.

Additionally, according to Table 13, the vitamin final activity seems to not experiment great variations. Therefore, the vitamin seems to be more resistant to changes in temperature and pressure than the enzyme.

Table 12: Maximum percent variation (%) in the BSAA final activity obtained by perturbing by $-\alpha\%$ and $+\alpha\%$ with α = 1, 5, 10 and 25 each decision parameter in the **Problem 2** solution (first row of Table 10).

Parameter	T_0	T_{r}	ΔP_1	ΔP_2	ΔP_3
±1%	16.9	15.1	1.8	7.4	6.8
±5%	31.8	33.5	12.9	10.6	6.3
±10%	52.6	21.6	11.7	31.5	8.0E-1
±25%	86.6	40.4	27.9	48.2	17.1
Parameter	ΔP_4	ΔP_5	ΔP_6	ΔP_7	ΔP_8
±1%	7.8E-1	3.2E-2	2.4E-2	2.0E-2	6.1E-3
±5%	5.9	6.2E-1	4.1E-2	5.6E-1	3.1E-2
±10%	3.9	6.8E-1	6.5E-2	5.7E-1	5.5E-2
±25%	3.9	7.4	4.2E-1	5.8E-1	2.7E-1

Table 13: Maximum percent variation (%) in the vitamin final activity obtained by perturbing by $-\alpha\%$ and $+\alpha\%$ with $\alpha = 1, 5, 10$ and 25 each decision parameter in the **Problem 3** solution (second row of Table 10).

Parameter	T_0	T_{r}	ΔP_1	ΔP_2	ΔP_3
$\pm 1\%$	5.6E-2	4.7E-2	1.0E-2	7.6E-3	9.9E-5
$\pm 5\%$	6.3E-2	3.6E-3	5.0E-2	4.2E-2	1.5E-3
$\pm 10\%$	1.6E-1	5.6E-2	1.0E-1	8.2E-2	2.1E-3
$\pm 25\%$	3.4E-1	7.5E-2	3.0E-1	2.2E-1	3.7E-3
Parameter	ΔP_4	ΔP_5	ΔP_6	ΔP_7	ΔP_8
$\pm 1\%$	9.6E-5	1.3E-6	3.6E-5	2.0E-5	2.7E-6
$\pm 5\%$	4.0E-3	6.6E-6	1.2E-3	1.1E-3	1.3E-5
$\pm 10\%$	5.5E-3	1.3E-5	1.6E-3	1.2E-3	2.6E-5
$\pm 25\%$	1.0E-2	3.3E-5	4.4E-3	2.1E-3	3.2E-4

5.5. Final improvement by using SD method

The methodology of using the WASF-GA to solve mono-objective problems can be improved by adding a last layer of local search. Once the most adequate point is selected for a particular mono-objective problem among the set of individuals belonging to the Pareto optimal front approximation, we propose to use the Steepest Descent (SD) method considering this point as an initial condition in a ten iterations process. For example, applying this idea to **Problem 2**, starting from the solution on Table 10 whose objective vector is $(f_{\mathrm{bsaa}}, f_{\mathrm{vit}}, f_{\mathrm{Tmax}}) = (0.2448, 0.9882, 49.85)$ associated to a cost function value of 0.2448, the final solution obtained has the following objective vector $(f_{\mathrm{bsaa}}, f_{\mathrm{vit}}, f_{\mathrm{Tmax}}) = (0.2405, 0.9881, 49.94)$ associated to a cost function value of 0.2405. For **Problem 3**, considering the individual corresponding to the objective vector $(f_{\mathrm{bsaa}}, f_{\mathrm{vit}}, f_{\mathrm{Tmax}}) = (0.3832, 0.9957, 46.57)$ (with a cost function value of 0.9957) as an initial condition, the SD method leads us to the solution with objective vector $(f_{\mathrm{bsaa}}, f_{\mathrm{vit}}, f_{\mathrm{Tmax}}) = (0.4000, 0.9959, 46.19)$ associated to a cost function value of 0.9959. We observe in both cases that the WASF-GA solutions have been improved by using the SD at the end of the algorithm. The extra time consumed by this added procedure is almost one hour.

6. Conclusions and future work

In this work, we have proposed a decision methodology based on multi-objective optimization to design High-Pressure Thermal processes for food treatment.

To this aim, first, the High-Pressure Thermal processing of solid type food has been modelled by coupling the heat transfer equation, to describe the evolution of the temperature and pressure in the food sample, with a kinetic equation, to model the effects of these physical magnitudes on the inactivation rate of each of the involved enzymes or vitamins. Then, this model has been incorporated

into an optimization procedure for determining the best configuration of a High-Pressure Thermal food treatment used to decrease the activity of the enzyme BSAA, preserve the activity of Vitamin C and avoid reaching high temperatures.

To tackle the optimization of such a food treatment, two approaches have been discussed. On the one hand, we have formulated some particular constrained mono-objective problems and solved them by applying a hybrid mono-objective algorithm called MLS-GA. On the other hand, we have considered a multi-objective optimization problem to be solved by using a preference-based optimization algorithm called WASF-GA. Once an approximate Pareto front of this multi-objective problem has been obtained by the WASF-GA, we have applied a decision strategy that consists of finding the point in this approximate solution that best solves a particular mono-objective optimization problem.

Then, we have compared both approaches by analyzing their solutions for different sets of parameters. Regarding the obtained results, we have observed that:

- The set of parameters denoted by A (corresponding to the highest crossover probability of 0.9 and the lowest mutation probability of 0.1, both with the distribution of 20.0 recommended in [10]) seems to be the most adequate for the WASF-GA and the considered optimization problems, as its associated solutions exhibited the best hypervolume value and, consequently, gave the best Pareto front approximation.

- The proposed decision methodology, applied to solve mono-objective constrained problems, achieved results similar to the MLS-GA ones. In some cases, it has found even better solutions than the MLS-GA.

- The presented decision methodology implies considerable savings in computational time as: i) it found solutions similar to the MLS-GA ones in less time (for example, MLS-GA with 27000 function evaluations needs almost twice the computational time, in average, than WASF-GA with 10800 function evaluations); ii) the same outcome obtained in a single run of the WASF-GA should be able to solve a large variety of mono-objective problems.

- The WASF-GA configured with 6600 function evaluations and the set of parameters A has produced, in a reduced computational time, a Pareto front approximation able to solve numerically the considered mono-objective problems.

- The solution obtained with our methodology can be improved by adding some iterations (here, 10) of the Steepest Descent method at the end of the algorithm.

Additionally, we have studied the optimal HPT configurations obtained as approximate solutions of the two particular mono-objective problems formulated previously. From those results, it seems that consistent with the common industrial procedure, an adequate strategy for treating the food sample consists

of increasing the pressure up to reaching the constrained temperature and, then, maintaining the pressure constant until the final pressure decreasing stage.

Finally, according to the sensitivity analysis of the decision parameters, it seems that the the initial and refrigeration temperatures have a great influence on the final enzymatic and vitamin activities. Therefore, the practitioners should intend to control perturbations in the temperatures during the implementation process. Moreover, imperfections of the pressure should not impact the general process performances.

In the future, we will research new mechanisms to improve the WASF-GA in order to deal with computationally expensive problems like the one concerning us. Furthermore, we will tackle the presented industrial problem increasing the number of objectives to incorporate more enzymes, vitamins or other properties of the food.

Acknowledgements

This research has been funded by grants from the Spanish Ministry of Economy and Competitiveness (TIN2015-66680-C2-1-R and MTM2015-64865P); Junta de Andalucía (P11-TIC7176 and P12-TIC301), in part financed by the European Regional Development Fund (ERDF). Juana López Redondo is a fellow of the Spanish "Ramón y Cajal" contract program, co-financed by the European Social Fund.

References

[1] R. Hayashi, Y. Kawamura, T. Nakasa, O. Okinaka, Application of high pressure to food processing: pressurization of egg white and yolk, and properties of gels formed, Agricultural and Biological Chemistry 53 (11) (1989) 2935–2939.

[2] A. Abakarov, Y. Sushkov, S. Almonacid, R. Simpson, Multiobjective optimization approach: thermal food processing, Journal of Food Science 74 (9) (2009) E471–E487.

[3] J. O. H. Sendín, A. A. Alonso, J. R. Banga, Efficient and robust multiobjective optimization of food processing: A novel approach with application to thermal sterilization, Journal of Food Engineering 98 (3) (2010) 317–324.

[4] K. Knoerzer, P. Juliano, P. Roupas, C. Versteeg, Innovative food processing technologies: advances in multiphysics simulation, John Wiley & Sons, 2011.

[5] A. Bisconsin-Junior, A. Rosenthal, M. Monteiro, Optimisation of high hydrostatic pressure processing of Pêra Rio orange juice, Food and bioprocess technology 7 (6) (2014) 1670–1677.

[6] S. Chakraborty, P. S. Rao, H. N. Mishra, Response Surface Optimization of Process Parameters and Fuzzy Analysis of Sensory Data of High Pressure–Temperature Treated Pineapple Puree, Journal of Food Science 80 (8) (2015) E1763–E1775.

[7] S. Bechikh, M. Kessentini, L. B. Said, K. Ghédira, Chapter Four - Preference Incorporation in Evolutionary Multiobjective Optimization: A Survey of the State-of-the-Art, Advances in Computers 98 (2015) 141–207.

[8] J. Branke, MCDA and Multiobjective Evolutionary Algorithms, in: Multiple Criteria Decision Analysis, Springer, 2016, pp. 977–1008.

[9] R. C. Purshouse, K. Deb, M. M. Mansor, S. Mostaghim, R. Wang, A review of hybrid evolutionary multiple criteria decision making methods, in: 2014 IEEE Congress on Evolutionary Computation, CEC'14), IEEE, 2014, pp. 1147–1154.

[10] A. B. Ruiz, R. Saborido, M. Luque, A preference-based evolutionary algorithm for multiobjective optimization: the weighting achievement scalarizing function genetic algorithm, Journal of Global Optimization 62 (1) (2015) 101–129.

[11] J. A. Infante, B. Ivorra, A. M. Ramos, J. M. Rey, On the Modelling and Simulation of High Pressure Processes and Inactivation of Enzymes in Food Engineering, Mathematical Models and Methods in Applied Sciences (M3AS) 19 (12) (2009) 2203–2229.

[12] W. Kowalczyk, A. Delgado, On convection phenomena during high pressure treatment of liquid media, High Pressure Research 27 (1) (2007) 85–92.

[13] L. Otero, A. M. Ramos, C. De Elvira, P. D. Sanz, A model to design high-pressure processes towards an uniform temperature distribution, Journal of Food Engineering 78 (4) (2007) 1463–1470.

[14] A. Delgado, C. Rauh, W. Kowalczyk, A. Baars, Review of modelling and simulation of high pressure treatment of materials of biological origin, Trends in Food Science & Technology 19 (6) (2008) 329–336.

[15] B. Guignon, A. M. Ramos, J. A. Infante, J. M. Díaz, P. D. Sanz, Determining thermal parameters in the cooling of a small-scale high-pressure freezing vessel, International Journal of Refrigeration 29 (7) (2006) 1152–1159.

[16] N. A. S. Smith, K. Knoerzer, A. M. Ramos, Evaluation of the differences of process variables in vertical and horizontal configurations of High Pressure Thermal (HPT) processing systems through numerical modelling, Innovative Food Science & Emerging Technologies 22 (2014) 51 – 62.

[17] S. Denys, L. R. Ludikhuyze, A. M. Van Loey, M. E. Hendrickx, Modeling Conductive Heat Transfer and Process Uniformity during Batch High-Pressure Processing of Foods, Biotechnology Progress 16 (1) (2000) 92–101.

[18] I. Indrawati, L. R. Ludikhuyze, A. M. Van Loey, M. E. Hendrickx, Lipoxygenase Inactivation in Green Beans (Phaseolus vulgaris L.) Due to High Pressure Treatment at Subzero and Elevated Temperatures, Journal of Agricultural and Food Chemistry 48 (5) (2000) 1850–1859.

[19] L. R. Ludikhuyze, I. Van den Broeck, C. A. Weemaes, M. E. Hendrickx, Kinetic Parameters for Pressure-Temperature Inactivation of Bacillus subtilis α-Amylase under Dynamic Conditions, Biotechnology Progress 13 (5) (1997) 617–623.

[20] E. M. T. Hendrix, B. G. Tóth, Introduction to Nonlinear and Global Optimization, Springer Optimization and Its Applications, 2010.

[21] K. Deb, K. Sindhya, J. Hakanen, Multi-objective optimization, in: Decision Sciences: Theory and Practice, CRC Press, 2016, pp. 145–184.

[22] B. Ivorra, B. Mohammadi, A. M. Ramos, A multi-layer line search method to improve the initialization of optimization algorithms, European Journal of Operational Research 247 (3) (2015) 711–720.

[23] D. G. Luenberger, Y. Ye, Linear and nonlinear programming, Vol. 228, Springer, 2015.

[24] A. M. Ramos, Introducción al análisis matemático del método de elementos finitos, Editorial Complutense, 2012.

[25] T. Norton, D. Sun, Recent Advances in the Use of High Pressure as an Effective Processing Technique in the Food Industry, Food and Bioprocess Technology 1 (1) (2008) 2–34.

[26] L. Otero, A. Ousegui, B. Guignon, A. Le Bail, P. D. Sanz, Evaluation of the thermophysical properties of tylose gel under pressure in the phase change domain, Food hydrocolloids 20 (4) (2006) 449–460.

[27] C. Hartmann, A. Delgado, J. Szymczyk, Convective and diffusive transport effects in a high pressure induced inactivation process of packed food, Journal of Food Engineering 59 (1) (2003) 33–44.

[28] L. Otero, A. D. Molina-García, P. D. Sanz, Some Interrelated Thermophysical Properties of Liquid Water and Ice. I. A User-Friendly Modeling Review for Food High-Pressure Processing, Critical Reviews in Food Science and Nutrition 42 (4) (2002) 339–352.

[29] L. Verbeyst, R. Bogaerts, I. Van der Plancken, M. Hendrickx, A. M. Van Loey, Modelling of vitamin C degradation during thermal and high-pressure treatments of red fruit, Food and Bioprocess Technology 6 (4) (2013) 1015–1023.

[30] J. J. Durillo, A. J. Nebro, jMetal: A Java framework for multi-objective optimization, Advances in Engineering Software 42 (2011) 760–771.

[31] L. While, L. Bradstreet, L. Barone, A fast way of calculating exact hypervolumes, IEEE Transactions on Evolutionary Computation 16 (1) (2012) 86–95.

[32] E. Zitzler, L. Thiele, Multiobjective optimization using evolutionary algorithms - a comparative case study, in: A. E. Eiben (Ed.), Parallel problem solving from nature V, Springer-Verlag, Amsterdam, 1998, pp. 292–301.

[33] M. Carrasco, B. Ivorra, A. M. Ramos, A variance-expected compliance model for structural optimization, Journal of optimization theory and applications 152 (1) (2012) 136–151.

[34] B. Ivorra, J. L. Redondo, J. G. Santiago, P. M. Ortigosa, A. M. Ramos, Two-and three-dimensional modeling and optimization applied to the design of a fast hydrodynamic focusing microfluidic mixer for protein folding, Physics of fluids 25 (3) (2013) 032001.

[35] B. Ivorra, B. Mohammadi, A. M. Ramos, Design of code division multiple access filters based on sampled fiber Bragg grating by using global optimization algorithms, Optimization and Engineering 15 (3) (2014) 677–695.

[36] M. Carrasco, B. Ivorra, A. M. Ramos, Stochastic topology design optimization for continuous elastic materials, Computer Methods in Applied Mechanics and Engineering 289 (2015) 131–154.

[37] B. Ivorra, J. L. Redondo, A. M. Ramos, J. G. Santiago, Design sensitivity and mixing uniformity of a micro-fluidic mixer, Physics of fluids 28 (1) (2016) 012005.

[38] M. Crespo, B. Ivorra, A. M. Ramos, A. Rapaport, Modeling and optimization of activated sludge bioreactors for wastewater treatment taking into account spatial inhomogeneities., Journal of Process Control 54 (2017) 118–128.

[39] S. Gomez, B. Ivorra, A. M. Ramos, Optimization of a pumping ship trajectory to clean oil contamination in the open sea, Mathematical and Computer Modelling 54 (12) (2011) 477 – 489.

[40] B. Ivorra, B. Mohammadi, P. Redont, L. Dumas, O. Durand, Semideterministic versus genetic algorithms for global optimisation of multichannel optical filters, International Journal of Computational Science and Engineering 2 (3-4) (2006) 170–178.